Electronic Supplementary Material (ESI) for CrystEngComm.

Supporting Information

Tailoring Surface Electron Configuration of Pt-Fe Alloy Electrocatalysts via a Wattecs Parallel Autoclave System Synthesis Technique for Promoting the Electrocatalytic Performance and Realizing Bifunctional Electrocatalysis

Guangran Xu,[a] Jiayin Liu,[a] Baocang Liu,[a,b] Xia Gong,[a] Shasha Wang,[a] Qin Wang,[a,b] and Jun Zhang [a,b]*

[a]College of Chemistry and Chemical Engineering, Inner Mongolia University, Hohhot 010021, P.R. China

[b]Inner Mongolia Key Lab of Nanoscience and Nanotechnology, Inner Mongolia University, Hohhot 010021, P.R. China

*Corresponding author: J. Zhang, Tel. & Fax: 0086 471 4995400, Email: cejzhang@imu.edu.cn

Table S1 The average particle size and the proportion of different crystal planes for Pt_3Fe(AA-HM), Pt_3Fe(Gly-HM), Pt_3Fe(HHA–HM), Pt_3Fe(AA–WPAS), Pt_3Fe(Gly–WPAS) and Pt_3Fe(HHA–WPAS) alloy nanoparticles deduced from XRD results.

Electrocatalysts	Particle size / nm	$I^{a}_{(200)/(111)}$	$I^{a}_{(220)/(111)}$
Pt_3Fe(AA-HM)	4.4	0.45	0.37
Pt_3Fe(Gly-HM)	5.6	0.43	0.27
Pt_3Fe(HHA-HM)	6.3	0.27	0.22
Pt_3Fe(AA-WPAS)	4.0	0.38	0.41
Pt_3Fe(Gly-WPAS)	4.9	0.45	0.29
Pt_3Fe(HHA-WPAS)	6.0	0.31	0.26

[a] The ratio of the peak intensity for the (200)/(111) and (220)/(111) crystal planes of Pt-Fe alloy nanoparticles

Table S2 The contents of Pt and Fe in different valence states on the surface of Pt-Fe alloy nanoparticles deduced from the XPS results.

Electrocatalyst	Atom ratio of Fe^{2+} to total Fe (%)	Atom ratio of Fe^{3+} to total Fe (%)	Atom ratio of Pt^{0} to total Pt (%)	Atom ratio of Pt^{2+} to total Pt (%)
Pt_3Fe(AA-HM)	34.2	65.8	82.5	17.5
Pt_3Fe(Gly-HM)	26.17	73.83	84.8	15.2
Pt_3Fe(HHA-HM)	15.83	84.17	85.32	14.68
Pt_3Fe(AA-WPAS)	40.92	59.08	82.69	17.31
Pt_3Fe(Gly-WPAS)	36.49	63.51	85.19	14.81
Pt_3Fe(HHA-WPAS)	29.73	70.27	91.42	8.58

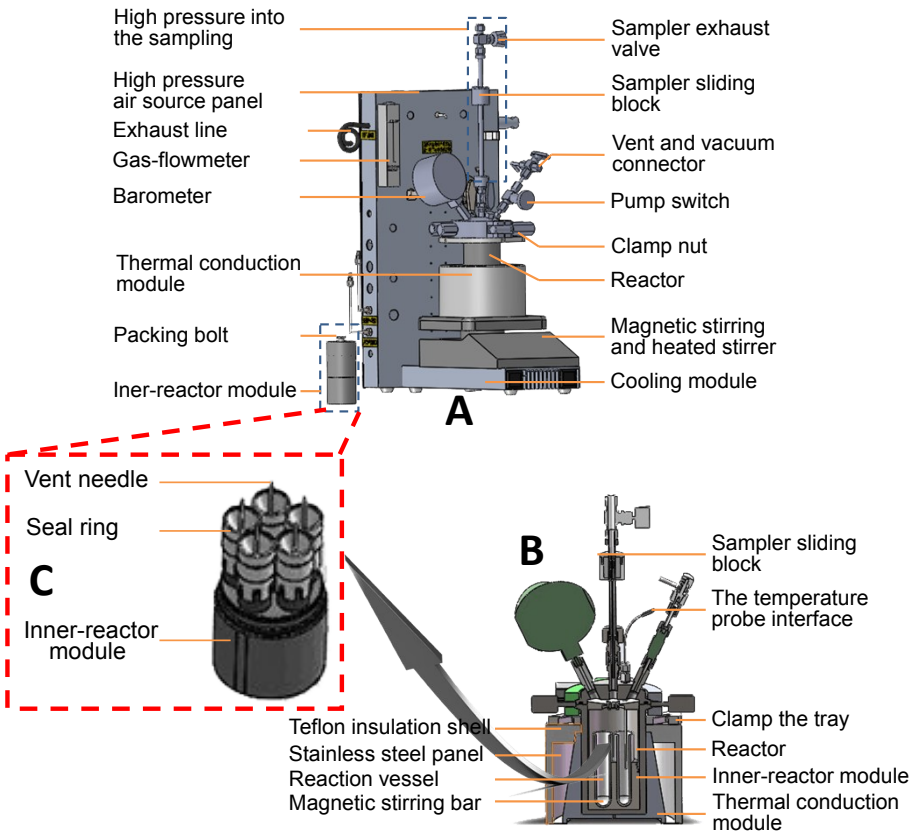

Scheme S1 (A) Over-view of WPAS; (B) Section-view of WPAS; (C) Diagram of the inner-reactor module of WPAS

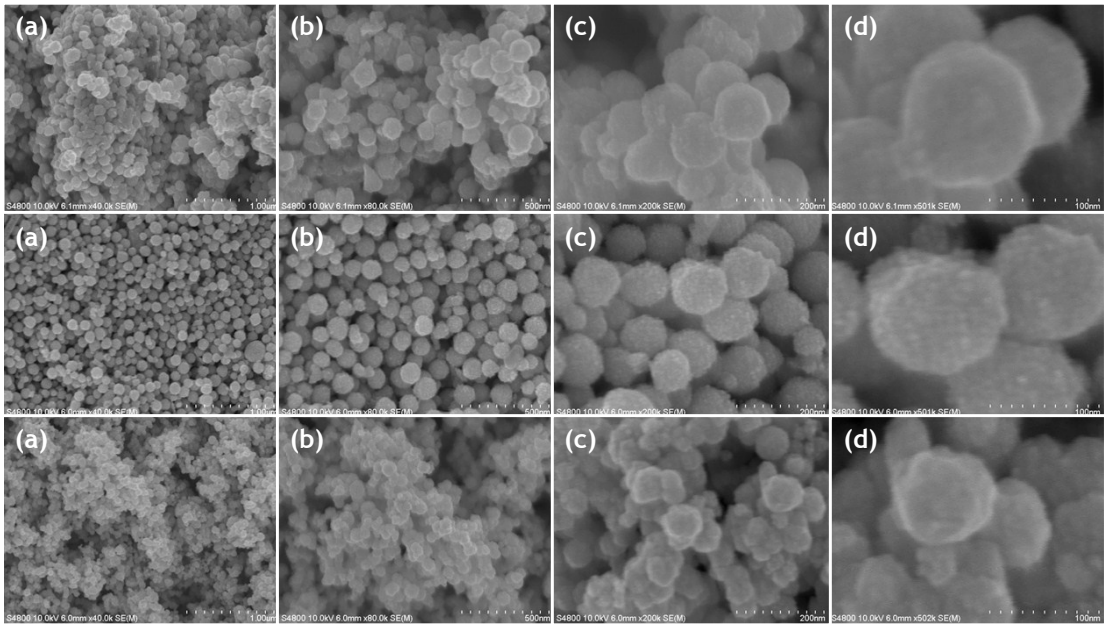

Fig. S1 SEM images of (a, b, c, and d) Pt_3Fe(AA-WPAS), (e, f, g, and h) Pt_3Fe(Gly-WPAS) and (i, j, k, and l) Pt_3Fe(HHA–WPAS) alloy nanoparticles.

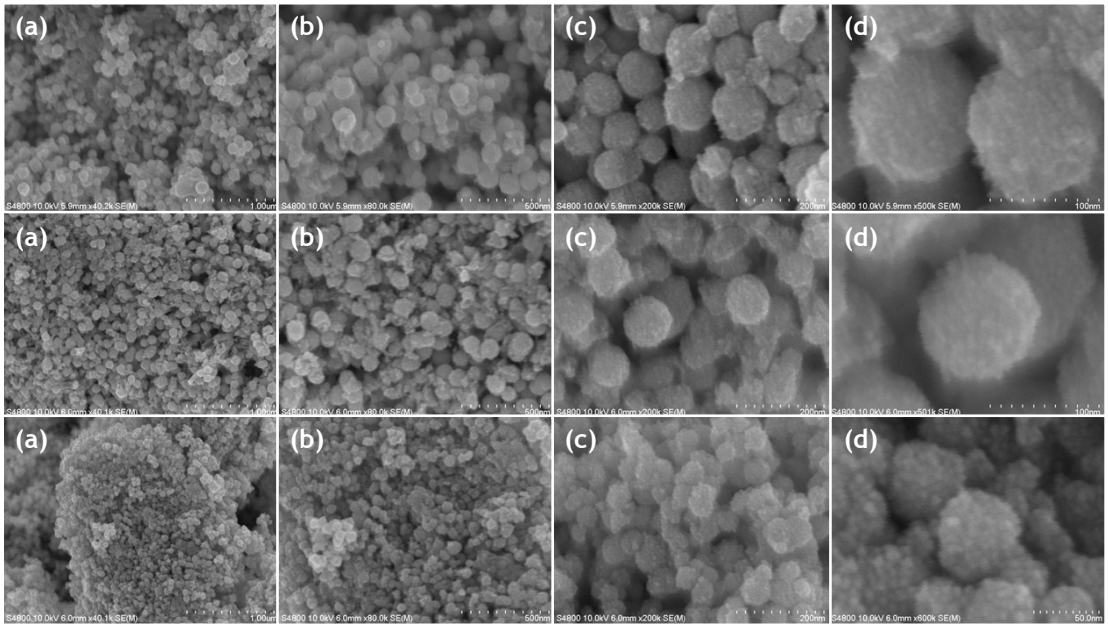

Fig. S2 SEM images of (a, b, c, and d) Pt_3Fe(AA-HT), (e, f, g, and h) Pt_3Fe(Gly-HT) and (i, j, k, and l) Pt_3Fe(HHA-HT) alloy nanoparticles.

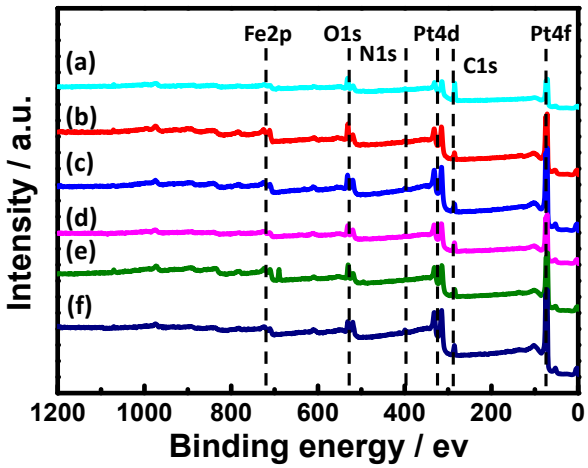

Fig. S3 Survey XPS spectra of (a) Pt_3Fe(AA-HT), (b) Pt_3Fe(Gly-HT), (c) Pt_3Fe(HHA–HT) (d) Pt_3Fe(AA–WPAS), (e) Pt_3Fe(Gly–WPAS), and (f) Pt_3Fe(HHA–WPAS) alloy nanoparticles.

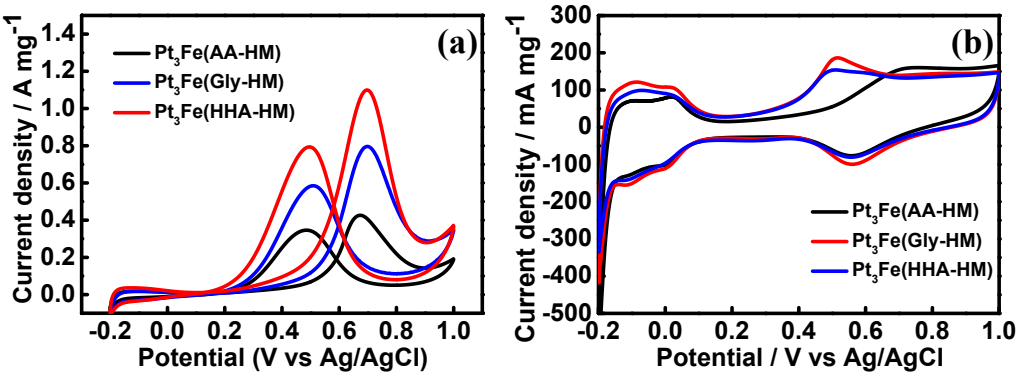

Fig. S4 (a) CV curves of Pt_3Fe(HT) alloy electrocatalysts measured in N_2 saturated 0.5 M H_2SO_4 solution at a scan rate of 100 mV s^{-1}; (b) CV curves of Pt_3Fe(HT) alloy electrocatalysts measured in N_2 saturated 0.5 M H_2SO_4 + 1.0 M CH_3OH solution at a scan rate of 50 mV s^{-1}.

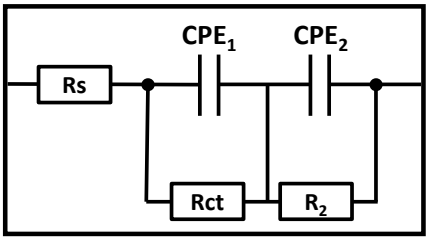

Fig. S5 The schematic representation of the electrical equivalent circuit diagram.

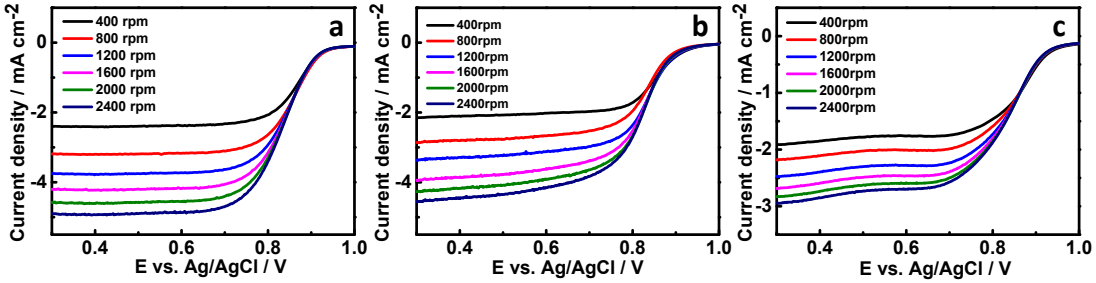

Fig. S6 ORR polarization curves of (a) Pt_3Fe(AA–HT), (b) Pt_3Fe(Gly–HT), and (c) Pt_3Fe(HHA–HT) alloy electrocatalysts in 0.1 M $HClO_4$